Static and Dynamic Properties of Quinoxalines in the Phosphorescent Triplet State from Optically Detected Magnetic Resonance

Kazuhiko SUGA and Minoru KINOSHITA*

The Institute for Solid State Physics, The University of Tokyo, Roppongi, Minato-ku, Tokyo 106

(Received August 27, 1981)

The static and dynamic properties of the phosphorescent triplet states of quinoxaline and 2,3-disubstituted derivatives in hexane have been studied at 1.4 K using the methods of optically detected magnetic resonance. In addition, the absorption and phosphorescence excitation spectra have also been measured to attain the information about the low lying excited states. A systematic comparison has been made for the purpose of examining the effect of substitution. A significant enhancement of the pumping rates for the y spin sublevel observed in the chlorine-substituted derivatives is concluded to be due to the additional indirect process of intersystem crossing which occurs from S_1 of n,π^* to T_1 passing through the intermediate triplet state of π,π^*. A detailed discussion on the observed phosphorescence spectra originating from the three sublevels has achieved a satisfactory success in understanding the mechanisms responsible for the radiative decay processes. It is concluded that the mechanisms due to vibronic coupling with closely lying n,π^* triplet states are of little importance in the systems studied here.

Quinoxaline is one of the most widely studied aza-aromatics from a variety of viewpoints. In particular, the properties of the lowest excited triplet state have attracted considerable attention[1-13] since the method of optically detected magnetic resonance (ODMR) was successfully applied to organic compounds.

Optical and magnetic resonance studies[5-13] have revealed that the interaction between the lowest π,π^* triplet state and low lying n,π^* states plays an important role in the decay and populating processes. However, with a few exceptions[12,13] the studies reported so far have little information on the detailed mechanisms, which give rise to the radiative decay from the individual spin sublevels.

Commonly, in order to obtain much information about the radiative activity of the spin sublevels at the vibronic bands, it is desirable to measure the phosphorescence spectra coming from the sublevels separately. Microwave-induced delayed phosphorescence (MIDP) method provides a useful procedure to obtain a sublevel emission spectrum. A set of three sublevel emission spectra makes it possible to discuss in detail the radiative properties even for the vibronic bands of small intensity.

In addition to quinoxaline, three 2,3-disubstituted quinoxalines are studied here in order to obtain closer insight into static and dynamic properties of the phosphorescent states by a systematical comparison. Besides the sublevel emission spectra, the kinetic rate constants are measured by means of the conventional MIDP method. The results are discussed in terms of the possible mechanisms of radiative transitions. The mechanisms operative in the intersystem crossing process are also discussed. The transition energies of the excited states are determined from the absorption and phosphorescence excitation spectra to provide supplementary information.

Experimental

Quinoxaline, 2,3-dimethylquinoxaline, 2-chloro-3-methylquinoxaline, and 2,3-dichloroquinoxaline were purified by recrystallization and vacuum sublimation. Hexane of spectroscopic grade obtained from Tokyo Kasei Co., Ltd. was used as received. The equipment and procedure for the optical and magnetic resonance experiments are essentially the same as described in previous papers.[14] The molecular structures and axis system for the compounds studied are shown in Fig. 1.

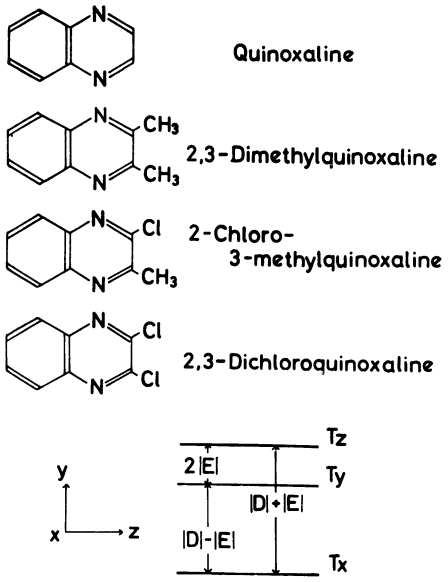

Fig. 1. Molecular structure and choice of axis system.

Absorption Spectra

The absorption spectra of quinoxaline and the three derivatives were measured in hexane at room temperature. The spectra are shown in Fig. 2.

Quinoxaline. As concerns quinoxaline, the analysis was based on the theoretical prediction about the transition energies and the moments for the transitions to the π,π^* excited singlet states reported in the literature.[15,16]

The first $^1A_1(\pi,\pi^*)$ band is observed with onset at 31490 cm^{-1}, and shows a slow decline, extending to $\cong$40000 cm^{-1}, which could be attributed to the presence of the second allowed π,π^* transition of B_2 symmetry. Accordingly, the peak found at 32780 cm^{-1} may be assigned as $^1B_2(\pi,\pi^*)$ band, predicted to lie at $\cong$32750 cm^{-1}.[15]

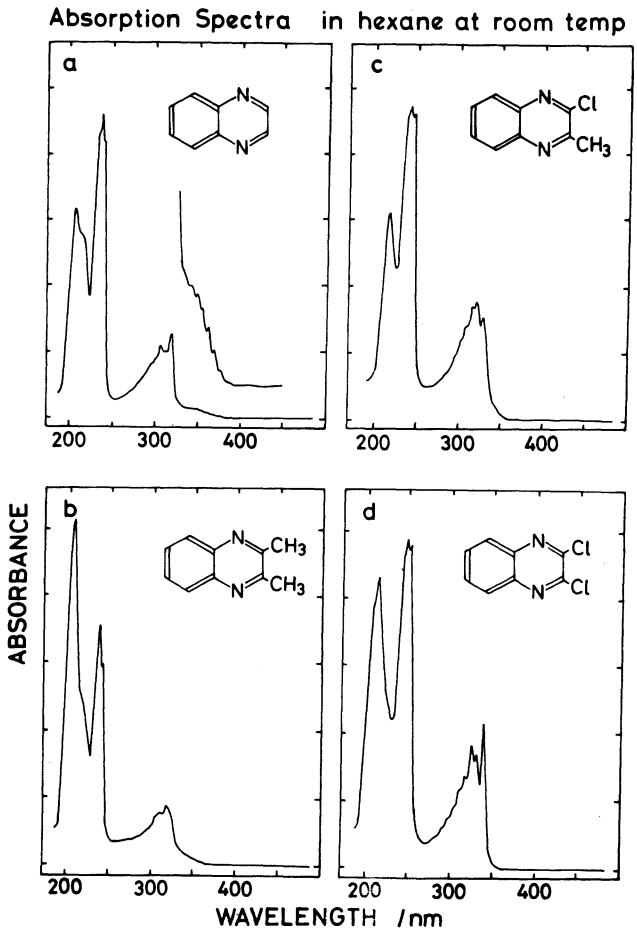

Fig. 2. The absorption spectra of quinoxalines in hexane at room temperature.
(a) Quinoxaline, (b) 2,3-dimethylquinoxaline, (c) 2-chloro-3-methylquinoxaline, and (d) 2,3-dichloroquinoxaline.

The second distinct structure is seen at 42720 cm^{-1} and, with reason, associated with the $^1A_1(\pi,\pi^*)$, which has been calculated to lie at 42670 cm^{-1}.[16] A more diffuse maximum is noted at ≅46930 cm^{-1} and followed by intense band with maximum at ≅49250 cm^{-1}. The former is likely attributed to the transition to the $^1B_2(\pi,\pi^*)$ state suggested to lie at ≅47200 cm^{-1} [15] and the latter to the $^1A_1(\pi,\pi^*)$ predicted at 49500 cm^{-1} [15] from the results of calculations.

In addition, the spectrum of quinoxaline contains a $^1B_1(n,\pi^*)$ transition at about 26300 cm^{-1}, which is in good agreement with the calculated value of 26382 cm^{-1}.[16] The electronic origin of this transition has been reported previously to lie at 25825 cm^{-1} in a naphthalene host crystal by Clarke *et al.*,[17] and at 27071 cm^{-1} in vapor phase by Glass *et al.*[18]

Substituted Quinoxalines. It is seen from Fig. 2 that the absorption spectra of the substituted quinoxalines are similar to that of quinoxaline. This apparent similarity permits the analysis to be made easily by comparison. The effect of substitution shifts the π,π^* excited singlet states to the red by a considerable amount.

It is to be noted that in the case of chloro-substituted quinoxalines, the absorption bands corresponding to the band at 46930 cm^{-1} of quinoxaline reduce the intensity significantly. In fact, the band in the spectrum of 2-chloro-3-methylquinoxaline is buried in the subsequent intense band, and the band in 2,3-dichloroquinoxaline is recognized only as a weak shoulder.

Phosphorescence Excitation Spectra

The phosphorescence excitation spectra of the four compounds were observed in hexane at 4.2 K. The spectra are shown in Fig. 3. It is seen from Figs. 2 and 3 that the lowest excited singlet states of all the three substituted quinoxalines are also of n,π^* character in hexane.

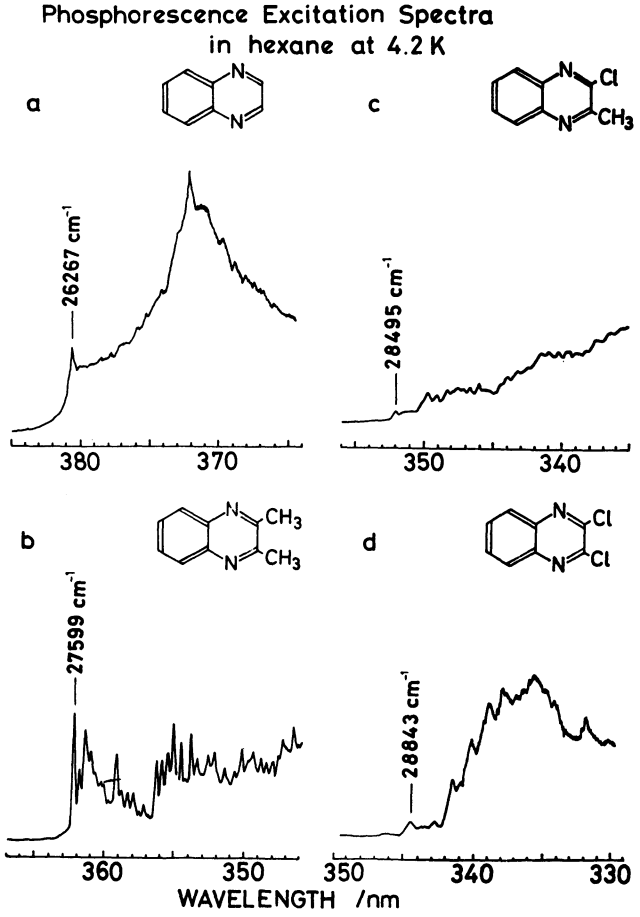

Fig. 3. The phosphorescence excitation spectra of quinoxalines in hexane at 4.2 K.
(a) Quinoxaline, (b) 2,3-dimethylquinoxaline, (c) 2-chloro-3-methylquinoxaline, and (d) 2,3-dichloroquinoxaline.

The phosphorescence excitation spectra of the neat crystals of quinoxaline and 2,3-dimethylquinoxaline were also measured as shown in Fig. 4. The first absorption bands in these excitation spectra correspond to the $^3B_2(\pi,\pi^*)\leftarrow S_0$ transitions. The absorption bands found at 24032 cm^{-1} in the spectrum of quinoxaline and at 25182 cm^{-1} in that of 2,3-dimethylquinoxaline are assigned to the $^3B_1(n,\pi^*)\leftarrow S_0$ transitions.

The energy separations between the $^1B_1$ and $^3B_1(n,\pi^*)$ states are very similar in these two compounds, and about 2350 cm^{-1}. By assuming that these states of all the compounds studied here are separated by the

Table 1. The energy levels of the excited electronic states of quinoxaline and the derivatives (in units of cm^{-1})

	Quinoxaline	2,3-Dimethyl-quinoxaline	2-Chloro-3-methyl-quinoxaline	2,3-Dichloro-quinoxaline
$^3B_2(\pi,\pi^*)$	21 325[a]	22 149[a]	21 885[a]	21 523[a]
$^3B_1(n,\pi^*)$	(23 920)[b]	(25 250)[b]	(26 150)[b]	(26 500)[b]
$^1B_1(n,\pi^*)$	26 267[c]	27 599[c]	28 495[c]	28 843[c]
$^1A_1(\pi,\pi^*)$	31 490	31 440	30 480	29 660
$^1B_2(\pi,\pi^*)$	32 780	32 250	31 790	31 000
$^1A_1(\pi,\pi^*)$	42 720	42 180	41 310	40 150
$^1B_2(\pi,\pi^*)$	46 930	46 280		45 440
$^1A_1(\pi,\pi^*)$	49 250	48 650	46 500	46 930

a) Obtained from the phosphorescence spectra at 4.2 K. b) The values in the parentheses are estimated ones, see text. c) Obtained from the phosphorescence excitation spectra at 4.2 K. Others were determined from the absorption spectra at room temperature.

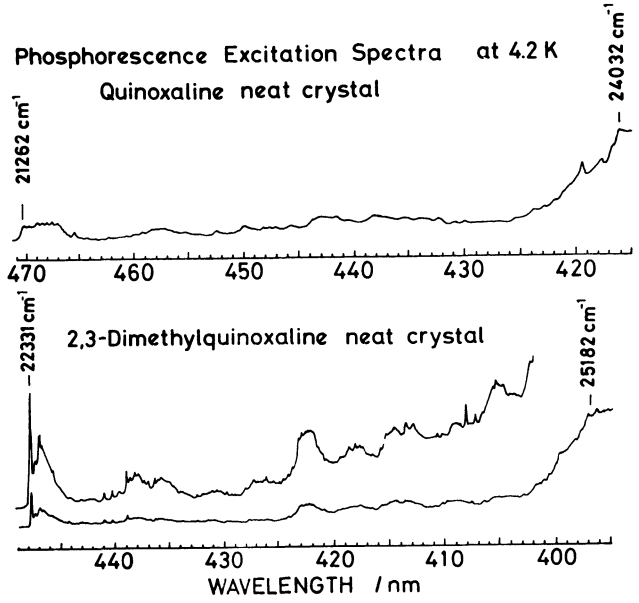

Fig. 4. The phosphorescence excitation spectra of (a) the quinoxaline neat crystal and (b) the 2,3-dimethylquinoxaline neat crystal at 4.2 K.

amount of 2350 cm^{-1}, the locations of $^3B_1(n,\pi^*)$ states are estimated. All the data for the locations of the excited states obtained from the absorption, phosphorescence excitation, and phosphorescence spectra are listed in Table 1.

ODMR Results

The zero-field (zf) transitions among the spin sublevels were measured to determine the zf splitting parameters D and E by means of the steady state phosphorescence microwave double resonance (PMDR) technique and/or the MIDP technique. The zf splitting parameters D and E are defined in a similar manner used commonly for naphthalene (Fig. 1). The total decay rates, k_i, steady state populations, N_i^0, and relative populating rates, P_i, for the spin sublevels (i=x, y, z) were also obtained by the MIDP method. The results for all the compounds are summarized in Table 2 for the sake of comparison.

Quinoxaline. Only two strong zf ODMR signals were observed by monitoring the phosphorescence emission in hexane. The signal at 1.157 GHz is assigned to the $T_z \leftrightarrow T_y$ transition, which has been observed at 1.187 GHz in a durene host[9] and at 1.132 GHz in a naphthalene-d_8 host.[9,13] The signal at 3.557 GHz is referable to the $T_z \leftrightarrow T_x$ transition, which has been found at 3.641 GHz in durene[9] and at 3.480 GHz in naphthalene-d_8.[9] The total decay rates obtained here are similar to those in durene[9] and naphthalene-d_8[9,13] reported by other authors.

2,3-Dimethylquinoxaline. The zf transitions are observed at 1.239 GHz for the $T_z \leftrightarrow T_y$ transition and at 3.731 GHz for $T_z \leftrightarrow T_x$. The total decay rates for all the three sublevels of 2,3-dimethylquinoxaline are

Table 2. The zero field splitting and kinetic parameters of quinoxaline and the derivatives

	Quinoxaline	2,3-Dimethyl-quinoxaline	2-Chloro-3-methyl-quinoxaline	2,3-Dichloro-quinoxaline
$\lvert D\rvert/cm^{-1}$	0.0993	0.1075	0.1017	0.1017
$\lvert E\rvert/cm^{-1}$	0.0193	0.0207	0.0189	0.0179
k_z/s^{-1}	12.3±0.3	7.23±0.14	3.54±0.09	3.29±0.12
k_y/s^{-1}	1.14±0.06	0.67±0.06	5.04±0.10	6.18±0.10
k_x/s^{-1}	0.86±0.02	0.34±0.03	0.45±0.03	0.38±0.01
N_z^0	1	1	1	1
N_y^0	0.90±0.08	0.99±0.06	0.80±0.05	0.78±0.05
N_x^0	0.64±0.07	1.61±0.15	0.82±0.06	0.48±0.03
P_b	1	1	1	1
P_y	0.084	0.091	1.14	1.45
P_z	0.045	0.075	0.10	0.055

smaller by a factor of about 0.6 than those of quinoxaline.

2,3-Dichloroquinoxaline. The observed zf transitions at 2.510 and 3.586 GHz can be assigned to the $T_y \leftrightarrow T_x$ and $T_z \leftrightarrow T_x$ transition, respectively, which have been reported to be at 2.467 and 3.515 GHz in a durene host crystal.[19,20] The total decay rates of the sublevels determined here are somewhat smaller than those obtained in other crystal systems.[19-22] It is to be noted that the relative populating rate of the y sublevel is as large as that of the z sublevel.

2-Chloro-3-methylquinoxaline. As in the case of 2,3-dichloroquinoxaline, the zf ODMR signals found at 2.483 and 3.616 GHz are attributed to the $T_y \leftrightarrow T_x$ and $T_z \leftrightarrow T_x$ transition, respectively. The total decay rate for the y sublevel is smaller to a certain extent than that of 2,3-dichloroquinoxaline, while with respect to the z and x sublevels, there is little difference between these compounds. The pattern of populating process is also characterized by high selectivity for both the z and y sublevels, as in the case of 2,3-dichloroquinoxaline.

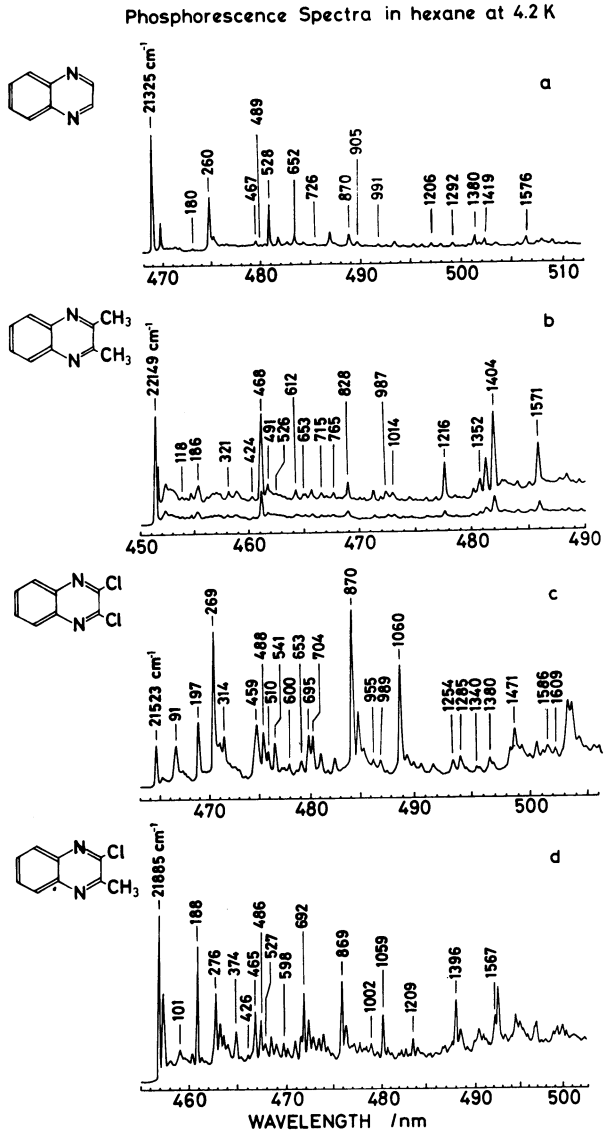

Fig. 5. The phosphorescence spectra in hexane at 4.2 K. (a) Quinoxaline, (b) 2,3-dimethylquinoxaline, (c) 2,3-dichloroquinoxaline, and (d) 2-chloro-3-methylquinoxaline.

Phosphorescence Spectra

The phosphorescence spectra of quinoxaline and the three derivatives in hexane are characterized by well resolved feature (FWHM=0.3 nm). The spectra obtained at 4.2 K are presented in Fig. 5. Assignments of the vibronic bands in the spectra were made in reference to the vibrational assignments of the IR and Raman spectra reported in the literature.[23-25]

Quinoxaline. The spectrum obtained in hexane differs from those observed in the naphthalene-d_8[13] and durene[7,10,12] host crystals. The vibronic bands at 180, 260, and 904 cm^{-1} from the origin appear with considerable intensity in hexane. However, the corresponding bands are far from being observable in the other host crystal systems.[7,10,12,13]

2,3-Dimethylquinoxaline. There is noticeable difference between quinoxaline and 2,3-dimethylquinoxaline. The intensity of the vibronic band at 0−467 cm^{-1} exceeds those of the vibronic bands such as 0−525 cm^{-1} involving totally symmetric vibrations, in contrast with quinoxaline.

2,3-Dichloroquinoxaline. There is some difference between the spectra obtained in hexane and in durene.[19,22] The vibronic bands observed at 197, 459, 510, and 695 cm^{-1} from the origin appear with considerable intensity in hexane, whereas in the durene host, these bands appear as nothing more than weak traces. The vibronic bands found at 0−197 and 0−695 cm^{-1} are due to the b_1 vibrations, corresponding probably to the frequencies of 180 and 725 cm^{-1} of quinoxaline. The band at 0−459 cm^{-1} is attributed to the vibronic band involving a_2 vibration corresponding to that of 647 cm^{-1} of quinoxaline. The remaining band at 0−510 cm^{-1} is assigned to the vibronic band due to totally symmetric vibration.

2-Chloro-3-methylquinoxaline. The frequencies of the vibrations appearing in the spectrum of 2-chloro-3-methylquinoxaline are in excellent correspondence to those in that of 2,3-dichloroquinoxaline. This enables one to readily analyze the vibrational structure by comparing the spectra of these compounds. It is to be noted that the origin band appears intensely in the spectrum of 2-chloro-3-methylquinoxaline, whereas in 2,3-dichloroquinoxaline, the intensity of the 0,0 band is quite small.

Sublevel Emission Spectra

The sublevel emission spectra of all the four molecules measured by means of the MIDP method are shown in Fig. 6. The relative radiative decay rates for the 0,0 and some vibronic bands of interest were also determined. The results are shown in Table 3, where experimental errors are estimated to be about ±20% for the k_x^r and k_y^r values larger than 0.02 and about +100—−50% for those less than 0.02. It is to be noted that the sublevel spectra in Fig. 6 show only the qualitative feature of the spin selectivity of each sublevel; in other

Table 3. Relative radiative decay rate constants for some vibronic bands

Band $\Delta\nu/cm^{-1}$	k_z^r	k_y^r	k_x^r	Assignment
		(a) Quinoxaline		
0	1	0.008	0.011	0,0
260	1	0.024	0.012	a_2 γ skel. dist.
467	1	0.013	0.018	a_2 γ skel. dist.
489	1	0.014	0.015	b_1 γ skel. dist.
528	1	0.007	0.015	a_1 β skel. dist.
652	1	0.012	0.020	a_2 γ skel. dist.
870	1	0.013	0.015	b_1 γ CH bend.
1056	1	0.009	0.018	528×2
		(b) 2,3-Dimethylquinoxaline		
0	1	0.032	0.049	0,0
186	1	0.024	0.059	b_1 ring wag.
424	1	0.031	0.064	b_1 γ skel. dist.
467	1	0.025	0.057	a_2 γ skel. dist.
612	1	0.039	0.060	a_1 β skel. dist.
828	1	0.033	0.061	b_2 β skel. dist.
1216	1	0.026	0.056	a_1 β CH bend.
1375	1	0.028	0.054	a_1 CH_3 sym. dist.
1404	1	0.029	0.046	a_1 β CH bend.
1571	1	0.032	0.032	a_1 β ring str.
		(c) 2,3-Dichloroquinoxaline		
0	1	0.29	0.07	0,0
91	1	10.2	0.30	a_2
197	1	0.35	0.09	b_1 ring wag.
269	1	12.7	0.26	a_2 γ skel. dist.
314	1	2.85	0.32	b_1
459	1	1.65	0.20	a_2 γ skel. dist.
488	1	1.17	0.26	b_1 γ skel. dist.
510	1	1.59	0.28	a_1 β skel. dist.
541	1	7.12	0.24	a_2
600	1	0.97	0.12	a_1 β skel. dist.
653	1	3.67	0.14	a_2
695	1	2.00	0.13	b_1 γ CH bend.
870	1	11.7	0.29	a_2 γ CH bend.
895	1	4.18	0.19	
1060	1	1.99	0.20	
		(d) 2-Chloro-3-methylquinoxaline		
0	1	1.56	0.13	0,0
101	1	5.00	0.35	$a''(a_2)$
188	1	1.39	0.19	$a''(b_1)$ ring wag.
276	1	5.88	0.35	$a''(a_2)$ γ skel. dist.
465	1	2.17	0.17	$a''(a_2)$ γ skel. dist.
486	1	2.44	0.24	$a''(b_1)$ γ kel. dist.
598	1	2.33	0.21	$a'(a_1)$ β skel. dist.
692	1	0.56	0.11	$a''(b_1)$ γ CH bend.
869	1	1.89	0.21	$a''(a_2)$ γ CH bend.
1059	1	1.20	0.20	
1396	1	1.56	0.14	$a'(a_1)$ β CH bend.
1567	1	0.79	0.13	$a'(a_1)$ β ring str.

a) The correlation of species of the C_s and C_{2v} symmetry groups is shown in the parentheses.

words, the spectra are not compatible with the data in Table 3, because some of the spectra were taken with different slit widths.

Brief comments on some of the specific experimental findings are described in the following.

Quinoxaline. It is clearly seen in Fig. 6(a) that the intensity of the vibronic bands such as 0—260, 0—904, 0—1380, and 0—1618 cm^{-1} relative to the 0,0 band is significantly larger in the y and x sublevel spectra than z. On the other hand, no spin state selectivity is noted with regard to the intensity of the bands such as 0—467, 0—527, 0—651, and 0—1576 cm^{-1}. The vibronic bands involving b_2 vibrations have a certain intensity in the y and x sublevel spectra.

2,3-Dimethylquinoxaline. The emission spectra of the spin sublevels resemble each other. It is found that the vibronic bands due to the b_1 vibrations such as 185, 424, and 490 cm^{-1} appear more intensely in all the three sublevel spectra in comparison with those of quinoxaline.

2,3-Dichloroquinoxaline. The vibronic bands involving a_2 or b_1 vibrations appear more strongly in all the three sublevel spectra than those of quinoxaline. On the other hand, the vibronic bands due to the b_2 vibrations have a considerable intensity only in the y sublevel spectrum. By examining carefully the change in the intensity, it is found that as concerns the y sublevel spectrum, the bands such as 0—269 cm^{-1} are affected by chlorine substitution to a more extent than the bands such as 0—459 cm^{-1}, although these vibrations are classified into the same species of a_2. With respect to the vibronic bands due to b_1 vibrations, a similar situation is found by comparing, for example, the bands at 0—197 and 0—488 cm^{-1}. This can be seen more clearly in Table 3(c).

2-Chloro-3-methylquinoxaline. Although both the a_2 and b_1 species in C_{2v} point group are reduced to the a″ species in C_s, the distinction between these species remains with regard to the radiative decay process, with an exception that the y sublevel emits strongly at the 0,0 band. This indicates clearly that the radiative decay process of 2-chloro-3-methylquinoxaline is governed by the mechanisms similar to those of 2,3-dichloroquinoxaline.

Assignments of Some Vibrations

Most of the vibronic bands in the phosphorescence spectra are assigned on the basis of the vibrational data reported previously[23-25] and confirmed by the experimental findings in the sublevel spectra. Several vibronic bands, however, are assigned anew. The bands such as 0—197 and 0—695 cm^{-1} of 2,3-dichloroquinoxaline are assigned only in view of the observed sublevel spectra. Here, the reasons for the assignments of the bands of importance are commented briefly.

Although no data of the vibrational assignments from IR and Raman spectra are available concerning the vibrations of 197 and 695 cm^{-1} of 2,3-dichloroquinoxaline, the vibronic bands due to these vibrations can be assigned to those of b_1 symmetry for the following reasons. First, the 0—197 cm^{-1} band appears with more intensity than the 0,0 band in the phosphorescence spectrum. Therefore, it is reasonable to leave the possibility of a_1 or b_2 species out of consideration. In fact, there are no vibrational modes of a_1 or b_2 species with such low frequency. Second, the behavior of this

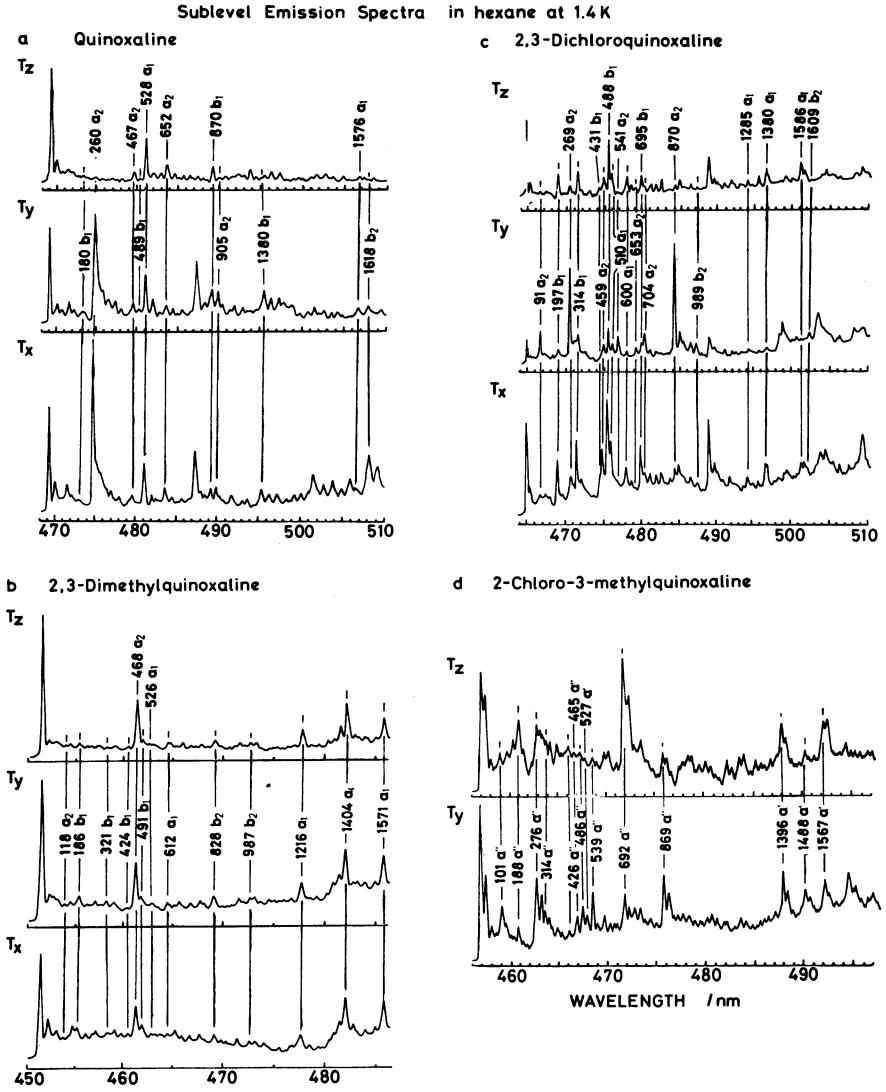

Fig. 6. The sublevel emission spectra in hexane at 1.4 K. (a) Quinoxaline, (b) 2,3-dimethylquinoxaline, (c) 2,3-dichloroquinoxaline, and (d) 2-chloro-3-methylquinoxaline.

band in the sublevel spectra is different from that of the vibronic band due to a_2 vibration such as 0—269 cm^{-1}, but rather similar to that of the band due to b_1 such as 0—488 cm^{-1}. The 0—695 cm^{-1} band can also be assigned to the band due to b_1 vibration in view of intensity behavior in the sublevel spectra. In fact, the corresponding band, 0—692 cm^{-1}, of 2-chloro-3-methylquinoxaline appears with much intensity in the z sublevel spectrum as well as the 0—188 cm^{-1} band corresponding to the 0—197 cm^{-1} band of 2,3-dichloroquinoxaline, but in contrast to the 0—276 cm^{-1} band corresponding to the 0—269 cm^{-1} band of 2,3-dichloroquinoxaline.

Electronic States

Some comments on the assignment of the low lying electronic states may be added, although the absorption and excitation spectra have been discussed briefly above. The absorption spectra of quinoxaline and 2,3-dichloroquinoxaline in hexane have been reported previously by another author.[26] The band at 42720 cm^{-1} of quinoxaline and the corresponding band at 40150 cm^{-1} of 2,3-dichloroquinoxaline have been assigned to the $^1B_2 \leftarrow S_0$ transition in the earlier works.[18,26] In the present study, however, these bands are assigned to the $^1A_1 \leftarrow S_0$ transition. This assignment is in good agreement with the theoretical predictions.[15,16]

It is again emphasized that the lowest excited singlet state is the $^1B_1(n,\pi^*)$ state for all the compounds studied here. Yamauchi and Azumi[22] have suggested that in a durene host the $^1B_1(n,\pi^*)$ state of 2,3-dichloroquinoxaline lies at 29520 cm^{-1}, higher by 1210 cm^{-1} than the $^1A_1(\pi,\pi^*)$ state, even though the transition monent for the transition to the $^1B_1$ state is considered to be much smaller than that to the $^1A_1$. On the other hand, the phosphorescence excitation spectrum of 2,3-dichloroquinoxaline in hexane obtained here shows that the $^1B_1(n,\pi^*)$ state lies lower than the $^1A_1$ state and is the lowest excited singlet state without question.

All the results for 2,3-dimethylquinoxaline and 2-chloro-3-methylquinoxaline are determined anew. The

locations of the $^3B_1$ states of quinoxaline and 2,3-dimethylquinoxaline are also determined from the present observation of the excitation spectra of the neat crystals.

The values of D are all very similar. They differ from each other only within 4%. The same holds true for the values of E. The methyl group and chlorine atom seem to have a little influence on the lowest excited triplet state with regard to the stationary properties of the wave function. Thus, it is reasonably assumed that (1) all the molecules studied here have essentially the same type of orbital wave function as that of the parent molecule, quinoxaline, and (2) there occurs no significant rotation of spin axes by going from the molecules with C_{2v} symmetry to the molecule with C_s. This latter point is strongly corroborated by the dynamic measurements. In fact, 2-chloro-3-methylquinoxaline shows the decay pattern similar to that of 2,3-dichloroquinoxaline.

Total Decay Rates

As for the z sublevel of aza-aromatics, the low lying n,π^* states are known to be of importance in the interactions relevant in causing both the radiative and radiationless decays.[1-5] Therefore, the decrease in k_z on substitution is presumably due to the reduction of the interaction with n,π^* states, resulting from the increased energy separations.

Quinoxaline and 2,3-dimethylquinoxaline show the relation of $k_z > k_y$. The decay process from the y sublevel is expected to be determined mainly by the interactions with n,π^* states.

On the other hand, in the case of chloro-substituted quinoxalines, the relation of $k_z < k_y$ indicates that there exists an additional mechanism for the decay from the y sublevel. The π electrons are likely to delocalize onto the chlorine atom(s) in some degree, so that one center integrals at the chlorine atom are expected to mean something to the spin orbit coupling matrix elements. Hence, the y sublevel can mix significantly with the $^1\sigma,\pi^*$ state *via* a one-center spin orbit coupling matrix element, in addition to the mixing with the ^{1}n,π^* state *via* a two-center spin orbit coupling matrix element. Accordingly, the large activity of the y sublevel in the decay process observed in 2-chloro-3-methylquinoxaline is also ascribed to the influence of chlorine substitution on the spin orbit interaction as stated before for 2,3-dichloroquinoxaline.[19,22]

Intersystem Crossing

It is seen from Table 2 that in the case of quinoxaline and 2,3-dimethylquinoxaline, the z sublevel is populated in much preference to the other sublevels *via* intersystem crossing from S_1. Considering that the lowest excited singlet states of these compounds are n,π^* states of B_1 symmetry, the high selectivity for the z sublevel with respect to the intersystem crossing process must be, as stated before,[8,9] a consequence of the efficient spin orbit coupling between the $^1B_1$(n,π^*) and $^3B_2(\pi,\pi^*)$ states, by way of which only the z sublevel is coupled directly.

The situation is quite different for the chlorosubstituted quinoxalines. The populating pattern of these compounds is characterized by highly selective intersystem crossing to both of the z and y sublevels. Seeing that the $^1B_1$(n,π^*) is the lowest excited singlet state, as observed above, the direct spin orbit coupling with S_1 accounts for P_z. The value of P_y is quite large for the chlorosubstituted derivatives as compared with that for quinoxaline and 2,3-dimethylquinoxaline. For a similar enhancement in the system of 2,3-dichloroquinoxaline in durene, Tinti and El-Sayed have suggested two possible mechanisms which differ depending on the assignment of the nature of the lowest excited singlet state.[19] On the basis of the present n,π^* assignment, these mechanisms can be discriminated unambiguously. The $^3A_1(\pi,\pi^*)$ state is expected to lie lower in energy than the $^1B_1$(n,π^*) state in the case of 2,3-dichloroquinoxaline, because chlorine substitution shifts π,π^* states to the red and n,π^* states to the blue, as mentioned above. Further, considering the n orbitals to be mixed with other σ orbitals of the aromatic frame (delocalization) to a certain extent, $^3A_1(\pi,\pi^*)$ state could couple with $^1B_1$(n,π^*) state appreciably. If this is the case, it is necessary to take into account an indirect process, which goes from S_1 through the intermediate triplet state, $^3A_1(\pi,\pi^*)$, and then to T_1. This process can populate only the y sublevel. Thus, the large value of P_y observed in 2,3-dichloroquinoxaline is surely ascribed to this additional intersystem crossing mechanism. The same holds true for 2-chloro-3-methylquinoxaline.

Mechanisms of Radiative Decay

As described above, all the molecules studied here are considered to have essentially the same type of orbital wave function. In the following discussion, therefore, it is assumed that all the molecules can well be characterized by C_{2v} point group symmetry for the purpose of avoiding unnecessary complications. Including up to the second order perturbations, the possible mechanisms, which are group-theoretically predicted, are divided into the following classes.[27]

(I) Spin orbit coupling.

(II) Vibronic coupling in the singlet manifold with spin orbit coupling.

(III) Spin orbit coupling with vibronic coupling in the triplet manifold.

(IV) Spin vibronic coupling.

Among a number of the mechanisms group-theoretically allowed, the mechanisms of little importance are excluded in view of the following criteria:

(1) Spin orbit, spin vibronic, and vibronic coupling operators are considered as the sum of one-electron operators in good approximation;

(2) As concerns mechanisms of types (II) and (III), the perturbing singlet configurations, which have allowed transitions to the ground state, are limited to π,π^*;

(3) With respect to mechanisms of type (IV), the contribution of the mechanisms involing $^3\pi,\pi^*$ and $^1\pi,\pi^*$ states is neglected because of the vanishingly small magnitude of the matrix elements between these states.

Table 4. All the possible mechanisms for the radiative decay process

Species[a]		Mechanism[b]
a_1	I.1	$T_z \leftarrow so \rightarrow {}^1B_1(n,\pi^*)$
	I.2	$T_z \leftarrow so \rightarrow {}^1B_1(\sigma,\pi^*)$
	I.3	$T_y \leftarrow so \rightarrow {}^1A_2(n,\pi^*)$
	I.4	$T_y \leftarrow so \rightarrow {}^1A_2(\sigma,\pi^*)$
	I.5	$T_x \leftarrow so \rightarrow {}^1A_1(\pi,\pi^*)$
a_2	II.1	$T_z \leftarrow so \rightarrow {}^1B_1(n,\pi^*) \leftarrow v \rightarrow {}^1B_2(\pi,\pi^*)$
	II.2	$T_z \leftarrow so \rightarrow {}^1B_1(\sigma,\pi^*) \leftarrow v \rightarrow {}^1B_2(\pi,\pi^*)$
	III.1	$T_z \leftarrow v \rightarrow {}^3B_1(n,\pi^*) \leftarrow so \rightarrow {}^1B_2(\pi,\pi^*)$
	III.2	$T_z \leftarrow v \rightarrow {}^3B_1(\sigma,\pi^*) \leftarrow so \rightarrow {}^1B_2(\pi,\pi^*)$
	II.3	$T_y \leftarrow so \rightarrow {}^1A_2(n,\pi^*) \leftarrow v \rightarrow {}^1A_1(\pi,\pi^*)$
	II.4	$T_y \leftarrow so \rightarrow {}^1A_2(\sigma,\pi^*) \leftarrow v \rightarrow {}^1A_1(\pi,\pi^*)$
	III.3	$T_y \leftarrow v \rightarrow {}^3B_1(n,\pi^*) \leftarrow so \rightarrow {}^1A_1(\pi,\pi^*)$
	III.4	$T_y \leftarrow v \rightarrow {}^3B_1(\sigma,\pi^*) \leftarrow so \rightarrow {}^1A_1(\pi,\pi^*)$
b_1	II.5	$T_z \leftarrow so \rightarrow {}^1B_1(n,\pi^*) \leftarrow v \rightarrow {}^1A_1(\pi,\pi^*)$
	II.6	$T_z \leftarrow so \rightarrow {}^1B_1(\sigma,\pi^*) \leftarrow v \rightarrow {}^1A_1(\pi,\pi^*)$
	III.5	$T_z \leftarrow v \rightarrow {}^3A_2(n,\pi^*) \leftarrow so \rightarrow {}^1A_1(\pi,\pi^*)$
	III.6	$T_z \leftarrow v \rightarrow {}^3A_2(\sigma,\pi^*) \leftarrow so \rightarrow {}^1A_1(\pi,\pi^*)$
	II.7	$T_y \leftarrow so \rightarrow {}^1A_2(n,\pi^*) \leftarrow v \rightarrow {}^1B_2(\pi,\pi^*)$
	II.8	$T_y \leftarrow so \rightarrow {}^1A_2(\sigma,\pi^*) \leftarrow v \rightarrow {}^1B_2(\pi,\pi^*)$
	III.7	$T_y \leftarrow v \rightarrow {}^3A_2(n,\pi^*) \leftarrow so \rightarrow {}^1B_2(\pi,\pi^*)$
	III.8	$T_y \leftarrow v \rightarrow {}^3A_2(\sigma,\pi^*) \leftarrow so \rightarrow {}^1B_2(\pi,\pi^*)$
	IV.1	$T_x \leftarrow sv \rightarrow {}^1B_1(n,\pi^*)$
	IV.2	$T_x \leftarrow sv \rightarrow {}^1B_1(\sigma,\pi^*)$
b_2	IV.3	$T_y \leftarrow sv \rightarrow {}^1B_1(n,\pi^*)$
	IV.4	$T_y \leftarrow sv \rightarrow {}^1B_1(\sigma,\pi^*)$
	II.9	$T_x \leftarrow so \rightarrow {}^1A_1(\pi,\pi^*) \leftarrow v \rightarrow {}^1B_2(\pi,\pi^*)$
	III.9	$T_x \leftarrow v \rightarrow {}^3A_1(\pi,\pi^*) \leftarrow so \rightarrow {}^1B_2(\pi,\pi^*)$

a) The first column shows the coupled vibrational species.
b) The interaction is indicated by the following notations: so, spin orbit coupling; v, vibronic coupling; sv, spin vibronic coupling.

Accordingly, the mechanisms, which are listed in Table 4, remain to be taken into consideration.

In the case of chloro-substituted quinoxalines, the π electron orbitals of the aromatic frame are mixed in some degree with the out-of-plane atomic orbital on the chlorine atom. This is responsible for the large red-shift of the π,π^* excited singlet states. This also causes the matrix elements of the spin orbit coupling to contain integrals over the chlorine atomic orbitals. Since σ orbitals are easily mixed with the in-plane orbitals of the chlorine atom, the matrix elements between π,π^* and σ,π^* states become large through one-center integrals on the chlorine atom. In view of the localized character of n orbitals, the integrals over the chlorine atomic orbitals make relatively small contribution to the matrix elements between π,π^* and n,π^* states. These points are to be kept in mind in the following discussion.

The 0,0 Band and Vibronic Bands Involving a_1 Vibrations. As seen in Table 3(a), the z sublevel has the largest radiative activity at the 0,0 band in the phosphorescence spectrum of quinoxaline. As suggested by other authors,[5-8,10-13] there is no doubt to conclude that the main mechanism, which accounts for the activity of the z sublevel at the 0,0 band, is mechanism (I.1). This is a consequence of not only the efficient spin orbit coupling from the one-center terms on the N atom, but also rather small energy separation between the ${}^3B_2(\pi,\pi^*)$ and ${}^1B_1(n,\pi^*)$ states.

In the case of substituted quinoxalines, the spin orbit interaction between the ${}^3B_2(\pi,\pi^*)$ and ${}^1B_1(n,\pi^*)$ states is expected to be reduced in response to the increase in the energy separation, ΔE_{ST}. If the magnitude of the spin orbit matrix element is assumed to be affected by no means on substitution, the mixing coefficient, $(<|H_{SO}|>/\Delta E_{ST})^2$, is predicted to decrease by factors of 0.81, 0.56, and 0.46 for 2,3-dimethyl-, 2-chloro-3-methyl-, and 2,3-dichloroquinoxaline, respectively. Although the radiative and radiationless parts in the total decay rates can not be strictly separated for the lack of quantum yield data for phosphorescence and triplet formation, the degree of reductions of the total decay rates k_z appears to be in good correlation with the values estimated above, presumably indicating that the mixing with the ${}^1B_1(n,\pi^*)$ state is also the main source of the radiative activity of substituted quinoxalines.

In the x sublevel spectrum, the 0,0 band can gain radiative character through the interaction with ${}^1A_1(n,\pi^*)$ state; mechanism (I.5). In view of the ratio k_x^r/k_z^r, the radiative decay rate constants of the x sublevel for the 0,0 band are found to increase to some degree on chlorine substitution. This increase is mainly a consequence of the decrease in the energy difference between ${}^3B_2(\pi,\pi^*)$ and ${}^1A_1(\pi,\pi^*)$, and the increase in the probability of the transition between the ${}^1A_1(\pi,\pi^*)$ and the ground state (see Fig. 2).

On the other hand, the influence of chlorine substitution significantly enhances the radiative activity of the y sublevel at the 0,0 band. Therefore, in the case of chloro-substituted quinoxalines, the major source, which gives rise to the radiative activity at the 0,0 band, is concluded to be mechanism (I.4), of which the matrix element contains one-center integrals over the chlorine atomic orbitals. The same explanation has been suggested by other authors for 2,3-dichloroquinoxaline.[22] The large intensity of the 0,0 band in the y sublevel spectrum of 2-chloro-3-methylquinoxaline is attributable to the reduction in molecular symmetry to C_s, where A_2 symmetry is reduced to A″. Unlike the chloro-substituted quinoxalines, mechanism (I.4) is expected to make a minor contribution, and mechanism (I.3) is likely to be the main one in the case of 2,3-dimethylquinoxaline, as stated for quinoxaline.[13] In fact, the rather small energy denominator and the large contribution of the N atomic orbital to the matrix element are in favor of mechanism (I.3).

The Vibronic Bands Involving a_2 Vibrations. For the vibronic bands due to a_2 vibrations, mechanisms (II.1), (II.2), (III.1), and (III.2) may contribute to the z sublevel emission. In the case of naphthalene, the bands of this type, which are exclusively due to the interaction involving σ,π^* states; mechanisms (II.2) and (III.2), have a negligible intensity in the spectrum.[28] Thus, it is reasonable to leave mechanisms (II.2) and (III.2) out of consideration.

If mechanism (III.1) plays an important role, the

intensity of these bands in the z sublevel spectrum in comparison to that of the 0,0 bands is expected to decrease significantly in response to the increase in the energy difference between the $^3B_2(\pi,\pi^*)$ and $^3B_1(n,\pi^*)$ states. If mechanism (II.1) is the case, in contrast, these bands will increase intensity to a certain extent.

It is easily seen that the bands due to a_2 vibrations appear in the z sublevel spectra of substituted quinoxalines with somewhat more intensity than those of quinoxaline. In an instant, this leads to the conclusion that mechanism (II.1) is the main source in producing the radiative activity of the z sublevel at the bands involving a_2 vibrations. The fact that the vibronic bands due to a_2 vibrations appear also in the $^1B_1(n,\pi^*)\leftarrow S_0$ absorption spectrum of quinoxaline in a naphthalene host crystal[17] strongly supports the validity of the inference described above.

With respect to the y sublevel, mechanisms (II.3), (II.4), (III.3), and (III.4) may make a contribution. An argument similar to that made concerning the z sublevel emission may explain the increase in intensity on chlorine substitution. The increase in intensity clearly indicates that mechanism (III.3) can not be of importance.

By examining the experimental results in detail, it is noticed that the vibronic bands such as 0−269, 0−541, and 0−870 cm^{-1} are enhanced by chlorine substitution more largely than the bands such as 0−459 and 0−653 cm^{-1}. This can also be seen from the relative radiative decay rate constants (see Table 4(c)). This difference in the enhancement can be understood in the following way. The former bands can be associated with mechanisms (II.4) and/or (III.4), in which the spin orbit matrix elements between σ,π^* and π,π^* states are affected strongly by the large one-center terms on the chlorine atom(s), whereas the latter bands can be due to mechanism (II.3), in which the contribution from the chlorine atom(s) is rather small.

The Vibronic Bands Involving b_1 Vibrations. The fact that naphthalene has no activity at the bands due to b_1 vibrations[28] evidently allows one to limit the possibility to mechanisms (II.5) and (III.5) with respect to the z sublevel. Since the bands of this type appear strongly in the chloro-substituted quinoxalines as compared with quinoxaline, there is no doubt to conclude that the z sublevel gains activity at these bands by mechanism (II.5). The increase in intensity can be ascribed to the decrease in the energy difference between the $^1B_1(n,\pi^*)$ and $^1A_1(\pi,\pi^*)$ states. In addition, the manifest evidence for the strong vibronic interaction between the $^1B_1$ and $^1A_1$ states has been found in the $^1B_1(n,\pi^*)\leftarrow S_0$ absorption spectrum reported previously.[17]

The detailed examination of the y sublevel emission reveals that the vibronic bands such as 0−197 cm^{-1} behave in different way from the bands such as 0−488 cm^{-1} with regard to the effect of chlorine substitution. Accordingly, by an argument similar to that made for the a_2 vibrations, it is possible to conclude that mechanisms (II.8) and/or (III.8) as well as (II.7) make a contribution toward producing the radiative activity at the bands due to b_1 vibrations.

The x sublevel emission is ascribed to either mechanisms (IV.1) or (IV.2). The experimental finding that the chlorine substitution affects the intensity to a great extent assuredly indicates that the x sublevel gains the radiative activity through mechanism (IV.2) in preference to (IV.1).

The Vibronic Bands Involving b_2 Vibrations. The vibronic bands due to b_2 vibrations are observable in the y and x sublevel emission. With regard to the y sublevel, mechanisms (IV.3) and (IV.4) may contribute. Of the two mechanisms, the former seems to be more favorable in view of the energy denominators. The intensity of the bands due to b_2 vibrations in the y sublevel emission is by no means affected by chlorine substitution. This seems to take a side with mechanism (IV.3).

Mechanisms (II.9) and (III.9) are predicted group-theoretically to contribute to the x sublevel emission. It is worthy to note that the configuration of the perturbing $^1B_2$ state is probably $\pi(b_1),\pi^*(a_2)$. Accordingly, the experimental finding that the bands due to b_2 vibrations appear in the spectrum of 2,3-dichloroquinoxaline with less intensity than in that of quinoxaline can be attributed to the decrease in the transition moment for the transition to the $^1B_2$ state, which is readily seen from the absorption spectra.

This work was partly supported by a Gran-in-Aid for Scientific Research from the Ministry of Education, Science and Culture (No. 510205).

References

1) M. S. de Groot, I. A. M. Hesselmann, J. Schmidt, and J. H. van der Waals, *Mol. Phys.*, **15**, 17 (1968).
2) D. M. Burland and J. Schmidt, *Mol. Phys.*, **22**, 19 (1971).
3) R. H. Clarke and J. M. Hayes, *J. Chem. Phys.*, **57**, 569 (1972); **59**, 3113 (1973).
4) D. A. Antheunis, J. Schmidt, and J.H. van der Waals, *Mol. Phys.*, **27**, 1521 (1974).
5) M. A. El-Sayed and R. G. Brewer, *J. Chem. Phys.*, **39**, 1623 (1963).
6) E. C. Lim and J. M. H. Yu, *J. Chem. Phys.*, **49**, 3878 (1968).
7) Y. Nakano and T. Azumi, *Bull. Chem. Soc. Jpn.*, **43**, 985 (1970).
8) S. M. Ziegler and M. A. El-Sayed, *J. Chem. Phys.*, **52**, 3257 (1970).
9) J. Schmidt, D. A.Antheunis, and J. H. van der Waals, *Mol. Phys.*, **22**, 1 (1971).
10) K. Ikegami and M. Ito, *Bull. Chem. Soc. Jpn.*, **45**,297 (1972).
11) R. Li and E. C. Lim, *J. Chem. Phys.*, **57**, 605 (1972).
12) S. Yamauchi and T. Azumi, *Chem. Phys. Lett.*, **21**, 603 (1973).
13) S. Yamauchi and T. Azumi, *J. Chem. Phys.*, **67**, 7 (1977).
14) E. Kanezaki, N. Nishi, and M. Kinoshita, *Bull. Chem. Soc. Jpn.*, **52**, 2836 (1979); K. Suga and M. Kinoshita, *ibid.*, **54**, 1651 (1981).
15) H. Baba and I. Yamazaki, *J. Mol. Spectrosc.*, **44**, 118 (1972).
16) J. E. Ridley and M. C. Zerner, *J. Mol. Spectrosc.*, **50**, 457 (1974).
17) R. H. Clarke, R. M. Hochstrasser, and C. J. Marzzacco, *J. Chem. Phys.*, **51**, 5015 (1969).

18) R. W. Glass, L. C. Robertson, and J. A. Merritt, *J. Chem. Phys.*, **53**, 3857 (1970).
19) D. S. Tinti and M. A. El-Sayed, *J. Chem. Phys.*, **54**, 2529 (1971).
20) D. Schweitzer, J. Zuclich, and A. M. Maki, *Mol. Phys.*, **25**, 197 (1973).
21) C. B. Harris and R. J. Hoover, *J. Chem. Phys.*, **56**, 2194 (1973).
22) S. Yamauchi and T. Azumi, *J. Chem. Phys.*, **68**, 4138 (1978).
23) W. L. F. Armerego, C. B. Barlin, and E. Spinner, *Spectrochim. Acta*, **22**, 17 (1966).
24) R. W. Mitchell, R. W. Glass, and J. A. Merritt, *J. Mol. Spectrosc.*, **36**, 310 (1970).
25) G. Peyronel, A. Pignedoli, and W. Malavosi, *Spectrochim. Acta, Part A*, **32**, 1015 (1976).
26) H. H. Perkampus, *Z. Naturforsch., A*, **17**, 614 (1962).
27) A. C. Albrecht, *J. Chem. Phys.*, **38**, 354 (1963).
28) D. M. Hanson, *J. Chem. Phys.*, **51**, 5063 (1969).